5101-281
Flat-Plate
Solar Array Project

DOE/JPL 1012-112
Distribution Category UC-63b

High-Efficiency Silicon Solar-Cell Design and Practical Barriers

Anant R. Mokashi
Taher Daud
Ram H. Kachare

November 15, 1985

Prepared for
U.S. Department of Energy
Through an Agreement with
National Aeronautics and Space Administration
by
Jet Propulsion Laboratory
California Institute of Technology
Pasadena, California

JPL Publication 85-75

TECHNICAL REPORT STANDARD TITLE PAGE

1. Report No. 85-75	2. Government Accession No.	3. Recipient's Catalog No.
4. Title and Subtitle High-Efficiency Silicon Solar-Cell Design and Practical Barriers		5. Report Date November 15, 1985 6. Performing Organization Code
7. Author(s) A. Mokashi		8. Performing Organization Report No.
9. Performing Organization Name and Address JET PROPULSION LABORATORY California Institute of Technology 4800 Oak Grove Drive Pasadena, California 91109		10. Work Unit No. 11. Contract or Grant No. NAS7-918 13. Type of Report and Period Covered JPL Publication
12. Sponsoring Agency Name and Address NATIONAL AERONAUTICS AND SPACE ADMINISTRATION Washington, D.C. 20546		14. Sponsoring Agency Code

15. Supplementary Notes Sponsored by the U.S. Department of Energy through Interagency Agreement DE-AI01-76ET20356 with NASA; also identified as DOE/JPL-1012-112 and as JPL Project No. 5101-281 (RTOP or Customer Code 776-52-61).

16. Abstract

A numerical evaluation technique is used to study the impact of practical barriers, such as heavy doping effects (Auger recombination, band gap narrowing), surface recombination, shadowing losses and minority-carrier lifetime (τ), on a high efficiency silicon solar cell performance. A hypothetical case, considering only radiative recombination losses and ignoring technology limited and fundamental losses is evaluated to estimate highest efficiency. Considering a high τ of 1 ms, efficiency of a silicon solar cell of the hypothetical case is estimated to be around 29%. This is comparable with (detailed balance limit) maximum efficiency of a p-n junction solar cell of 30%, estimated by Shockley and Queisser. Value of τ is varied from 1 second to 20 μs. Heavy doping effects, and realizable values of surface recombination velocities and shadowing, are then considered in succession and their influence on cell efficiency is evaluated and quantified. It is shown that these practical barriers cause the cell efficiency to reduce from the maximum value of 29% to the experimentally achieved value of about 19%. Improvement in open circuit voltage (V_{oc}) is required to achieve cell efficiency greater than 20%. Increased value of τ reduces reverse saturation current and, hence, improves V_{oc}. Control of surface recombination losses becomes critical at higher V_{oc}. Substantial improvement in τ and considerable reduction in surface recombination velocities is essential to achieve cell efficiencies greater than 20%.

17. Key Words (Selected by Author(s))	18. Distribution Statement
Power Sources Crystallography Solid-state physics	Unclassified-unlimited

19. Security Classif. (of this report)	20. Security Classif. (of this page)	21. No. of Pages	22. Price
Unclassified	Unclassified	32	

5101-281
Flat-Plate
Solar Array Project

DOE/JPL 1012-112
Distribution Category UC-63b

High-Efficiency Silicon Solar-Cell Design and Practical Barriers

Anant R. Mokashi
Taher Daud
Ram H Kachare

November 15, 1985

Prepared for
U S Department of Energy
Through an Agreement with
National Aeronautics and Space Administration
by
Jet Propulsion Laboratory
California Institute of Technology
Pasadena, California

JPL Publication 85-75

Prepared by the Jet Propulsion Laboratory, California Institute of Technology, for the U S Department of Energy through an agreement with the National Aeronautics and Space Administration

The JPL Flat-Plate Solar Array Project is sponsored by the U S Department of Energy and is part of the Photovoltaic Energy Systems Program to initiate a major effort toward the development of cost-competitive solar arrays

This publication reports on work done under NASA Task RE-152, Amendment 66, DOE / NASA IAA No DE-AI01-76ET20356

ABSTRACT

A numerical evaluation technique is used to study the impact of practical barriers, such as heavy doping effects (Auger recombination, band gap narrowing), surface recombination, shadowing losses and minority-carrier lifetime (τ), on a high efficiency silicon solar cell performance. A hypothetical case, considering only radiative recombination losses and ignoring technology limited and fundamental losses is evaluated to estimate highest efficiency. Considering a high τ of 1 ms, efficiency of a silicon solar cell of the hypothetical case is estimated to be around 29%. This is comparable with (detailed balance limit) maximum efficiency of a p-n junction solar cell of 30%, estimated by Shockley and Queisser. Value of τ is varied from 1 second to 20 μs. Heavy doping effects, and realizable values of surface recombination velocities and shadowing, are then considered in succession and their influence on cell efficiency is evaluated and quantified. It is shown that these practical barriers cause the cell efficiency to reduce from the maximum value of 29% to the experimentally achieved value of about 19%. Improvement in open circuit voltage (V_{OC}) is required to achieve cell efficiency greater than 20%. Increased value of τ reduces reverse saturation current and, hence, improves V_{OC}. Control of surface recombination losses becomes critical at higher V_{OC}. Substantial improvement in τ and considerable reduction in surface recombination velocities is essential to achieve cell efficiencies greater than 20%. Lack of available data for minority-carrier mobility, heavy doping effect, τ in thin emitters, surface recombination velocities, etc., are discussed. Limitations of one dimensional numerical analysis for considering two and three dimensional cell designs, such as floating emitter and dot junction cells, are pointed out.

ACKNOWLEDGEMENT

The authors would like to thank Andrew D. Morrison, Martin H. Leipold, K. M. Koliwad, and William T. Callaghan of the Flat-Plate Solar Array Project for their encouragement and support during this study.

CONTENTS

Figures

Tables

SECTION I

INTRODUCTION

As of today, the highest silicon solar cell efficiency practically realized is about 19% under 100 mW/cm^2 illumination (References 1 and 2). It is achieved by using best quality substrate and incorporating known high efficiency design features to enhance current collection and to reduce reverse saturation current, thereby improving V_{oc}. Some interesting questions to be answered are the following: what is the ultimate performance limit for crystalline silicon solar cells, what are the practical barriers, how much do these barriers influence in limiting the cell performance individually and collectively, and can these effects be quantified? Some of the earlier studies performed, that answered these questions partially, are briefly described below. Subsequently, the method followed during this study is presented.

The approach followed in the past for estimating the efficiency limits are classified into two categories, namely theoretical (References 3 through 5) and semiempirical (References 6 and 7). A hypotnetical semiconductor material is considered in the theoretical approach and cell efficiency as a function of band gap is estimated taking into account only the radiative recombination, as required by the principle of detailed balance and ignoring all other fundamental loss mechanisms (such as heavy doping effects). This gives the limiting efficiency known as the detailed balance limit of efficiency. Assuming the sun and a p-n junction silicon (band gap 1.1 eV) solar cell to be black bodies at temperatures of 6000°K and 300°K, respectively, Shockley and Queisser (Reference 3) have estimated the maximum efficiency of about 30%. In the semiempirical approach, a particular design with known material properties is considered and efficiency estimate is based on empirical values for the constants describing the characteristics of the solar cell. The efficiency limit predicted by this approach is known as the semiempirical limit.

The detailed balance limit approach has the weakness of neglecting fundamental loss mechanisms such as Auger recombination. Similarly in the semiempirical approach, being based on a particular design, the device dependent losses, in principle, can be eliminated by innovative designs.

The detailed balance limit of efficiency is expressed as a function of four variables, namely X_g, X_c, t_s and f, which in turn depend upon other parameters defined below. X_g and X_c are the ratios involving the three parameters, namely:

E_g = the energy gap of the semiconductor

T_s = temperature of the sun

T_c = temperature of the cell

and are expressed as

$$\chi_g = E_g/kT_s \tag{1}$$

and

$$\chi_c = T_c/T_s \tag{2}$$

where k is Boltzmann's constant.

The term t_s is defined as the probability that a photon with energy greater than E_g incident on the surface will produce a hole-electron pair, and f is defined as

$$f = f_c\ f_w\ t_s/2t_c \tag{3}$$

where

f_c = radiative recombination as a fraction of total recombination

f_w = the geometrical factor dependent upon the solid angle subtended by the sun and the angle of incidence upon the solar cell

t_c = probability that an incident photon of energy greater than E_g will enter the body and produce a hole-electron pair

The factor 2 (Equation 3) comes from the fact tnat sunlight falls only on one of the two cell surfaces.

Considering a perfectly absorbing cell ($t_s = t_c = 1$) with normal incidence ($f_w = w_s/\pi$), radiative recombination only ($f_c = 1$), $T_s = 6000^oK$ and $T_c = 300^oK$, the maximum efficiency is estimated to be 30% for p-n junction silicon solar cell. For this cell the ultimate efficiency considering $T_s = 6000^oK$, $T_c = 0^oK$ and f = 1 is estimated to be 44%.

Similarly, a general expression is derived by Mathers (Reference 5) for the upper limit of efficiency without assuming any specific device structure and the spectrum of the incident radiation or the absorption characteristics of the cell. The detailed balance limit derived for p-n junction cell (Reference 3) is shown to be a special case of this general result.

Tiedje, et al. (Reference 8), have extended the detailed balance method to include free carrier absorption and Auger recombination in addition to radiative losses. The limiting efficiency is found to be 29.8% under 100 mW/cm^2, based on measured optical absorption spectrum and published values of the Auger and free-carrier absorption coefficients.

In this study, we have used a one-dimensional numerical analysis technique to evaluate the performance of a given silicon solar cell design. This method uses all the device-based data as input. All the practical barriers which

are responsible for the semiempirical limit are also considered. The same method is used for estimating the ideal case ignoring all the other losses except the Shockley-Read-Hall (SRH) (References 9 and 10) recombination, which gives an approximation for a theoretical limit. The impact of practical barriers is estimated and quantified by taking them into account, one-by-one, in sequence.

Numerical analysis procedure and the base case design considered for analysis are described in Section II. Estimation of maximum efficiency approaching the theoretical limit and the gradual reduction of efficiency by introduction of practical barriers (such as Auger recombination, band-gap narrowing, and surface recombination velocities) is discussed in Section III. Limitations of the one-dimensional code in analyzing complicated cell designs, and lack of reliable experimental data and measurement techniques are described in Section IV and the study is summarized in Section V.

SECTION II

NUMERICAL EVALUATION

An accurate, sophisticated numerical analysis program (Reference 11) is used in this study as a basic tool for evaluating the performance of a silicon solar cell of a given design. A high efficiency cell design, based on our earlier studies (References 12 and 13), is used as an example for analyzing the impact of practical barriers on cell performance. The simulation program and the base case design are briefly described below.

A. SIMULATION PROGRAM

Solar Cell Analysis Program in 1-Dimension (SCAP1D) of Purdue University (Reference 11) is the simulation program used in this study. Mathematical model used in SCAP1D consists of Poisson's equation, electron continuity equation, and hole continuity equation; along with the electron and hole transport equations, which consider heavy doping effects such as nonuniform band structure and influence of Fermi-Dirac statistics. Two parameters, namely, effective band-gap shrinkage (ΔEg), and effective asymmetry factor (γ), account for the heavy doping effects. The empirical band-gap narrowing model developed by Slotboom and De Graaff (Reference 14) is used for calculating ΔEg. Solar cell performance parameters, V_{oc}, short circuit current density (J_{sc}), fill factor (FF), and efficiency (η) are calculated with an arbitrary choice for the value of γ (Reference 15) between 0 and 1. (Normally, $\gamma \simeq 0.5$ is used). Other phenomenological submodels incorporated in SCAP1D include the following: an empirical formula for the wavelength dependence of the absorption coefficient developed by Rajkanan, et al., (Reference 16); the doping dependent mobility from the empirical formula of Caughey and Thomas (Reference 17); and Auger recombination coefficients (band-to-band) from the measurements of Dziewior and Schmid (Reference 18).

A solar cell is divided into a large number of nonuniform grid points along the cell thickness, and the set of three differential equations are solved numerically by conventional finite difference technique. The solution gives the values of hole concentration (p), electron concentration (n) and electrostatic potential (v) as a function of position (along the cell thickness). Knowing p, n and v, cell performance parameters V_{oc}, J_{sc}, FF and η are computed.

Doping and geometric details of the design are specified by the user. τ and surface recombination velocities are also specified. User has a choice of considering Auger recombination and/or band-gap narrowing. Any of the design parameters can be altered individually or collectively for performing sensitivity analysis.

B. HIGH PERFORMANCE SILICON SOLAR CELL DESIGN

Since the current collection efficiency in cells has reached a near optimum level, improvement in silicon solar cell performance is possible by increase of V_{oc} (Reference 2). Reduction of reverse saturation current

density (J_o) will result in enhancement of V_{oc}. Recombination losses throughout the cell must be minimized to reduce J_o. Innovative design features are used to reduce the influence of loss mechanisms.

Surface recombination losses are reduced by passivating the surfaces with a thermally grown oxide layer. Attempts are made to reduce the recombination losses under the ohmic contact by providing a thin oxide layer below the contact and establishing the contact by quantum mechanical tunneling (Reference 1). Reducing the contact area is another approach (Reference 2). Providing a highly doped polysilicon layer under the contact is yet another method of controlling the recombination losses under the contact (Reference 13), which is presently under investigation.

The cell is made thin for reduction of bulk recombination losses. However, it has an adverse effect on optical absorption. Back surface reflector is therefore provided to effectively double the physical thickness to reduce the optical absorption loss.

A thin passivated silicon solar cell design, with back surface reflector, has been evaluated in our earlier study (Reference 13). It has been shown that a cell with 0.2 Ω-cm substrate resistivity, 100 μm thickness with front and back surface recombination velocities of 1000 cm/s and τ = 20 μs is capable of achieving 20% cell efficiency. In order to achieve cell efficiency greater than 20%, all recombination losses should be reduced to the extent that the total of J_o is less than 2×10^{-13} A/cm^2 (Reference 19). Many design configurations would satisfy this requirement.

One such passivated thin cell design is considered as an example for the base case in our present study. Analyses of the impact of practical barriers on efficiency of the base case design are presented in Section III.

SECTION III

IMPACT OF PRACTICAL BARRIERS ON SILICON SOLAR CELL PERFORMANCE

Base case design parameters of a passivated thin silicon solar cell, analyzed in this study, are given in Table 1. Schematic cross section of this design is shown in Figure 1. A 0.1 Ω-cm, p-type, 100 μm thick substrate with a 0.2 μm diffused n^+-region forms the cell. The τ in the base is assumed to be 250 μs. Both the front and back surfaces have contacts through etched windows in thermally grown passivated oxide. As shown in Figure 1, these contacts consist of thin, highly doped polycrystalline silicon on both surfaces under the Ti-Pd-Ag metal grid on the front and under an aluminum layer followed by Ti-Pd-Ag evaporation on the back. The aluminum layer adjacent to the 100 Å thick oxide layer also acts as the back surface reflector. The combined surface passivation of the open surfaces, and that under the contact with the use of polycrystalline silicon, is assumed to result in an effective recombination velocity at the front (SF) and at the back surface (SB) of about 100 cm/s. This cell is evaluated to achieve 21.59% cell efficiency with V_{oc} = 696 mV, J_{sc} = 36.71 mA/cm^2, and FF = 0.845.

Further an ideal case is analyzed in which only the SRH recombination is considered. All other loss mechanisms such as Auger recombination, band-gap narrowing effects, etc., are ignored. Technology limited barriers, such as SF, SB and shadowing (including reflection), are assumed to have zero values. The efficiency for this ideal case is evaluated with τ as a parameter. Practical barriers such as heavy doping effects (Auger recombination, and band gap narrowing), surface recombination velocities and shadowing are then introduced sequentially and the cell performance is evaluated. The impact of these barriers are quantified individually and collectively, and a detailed discussion is presented in this section.

A. MINORITY-CARRIER LIFETIME (τ)

The τ in the bulk is directly associated with recombination processes as a result of crystal imperfections, such as point defects and dislocations, or due to chemical impurities. In principle, these recombination mechanisms can be eliminated, almost completely, in a perfect crystal. Auger recombination and band-gap narrowing are fundamental mechanisms and are unavoidable. To develop high-efficiency cells it is necessary to have high purity material with high lifetimes. For the ideal case, considering only SRH recombination, the cell performance is dependent only on τ. In this study, the value of τ is varied over a wide range from 1 second to 20 μs and the cell performance parameters are presented in Table 2. Considering the τ value of 1 ms, the efficiency estimated is 29.02% (V_{oc} = 831 mV, J_{sc} = 40.56 and FF = 0.861), which is comparable with the theoretical limit for a p-n junction silicon solar cell of 30% estimated by Shockley and Queisser (Reference 3) and Mathers (Reference 5). For τ value of 1 second, the corresponding efficiency is 38.2% (V_{oc} = 1146 mV, J_{sc} = 40.59 mA/cm^2, FF = 0.821). It is observed from Table 2 that, for the variation of τ from 1 ms to 1 s, the improvement in efficiency is mainly due to increase in V_{oc} as a result of reduction in reverse saturation current density. It is also observed from Table 2, that

Table 1. Passivated Thin Silicon Solar Cell Design Parameters

Doping Profile:	Complimentary Error Function
Front Surface Doping:	$1.0 \times 10^{18}/cm^3$
Front Junction Depth:	$0.2\,\mu m$
Shadowing (including reflection):	7%
Bulk Doping (B):	$5 \times 10^{17}/cm^3$
Cell Thickness:	$100\,\mu m$
Back Surface Reflector:	Provided
Illumination:	100 mW/cm^2 (AM 1.5)

Additional Parameters Used for Numerical Evaluation

Minority-Carrier Lifetime in the Base:	$250\,\mu s$
Front Surface Recombination Velocity (SF):	100 cm/s
Back Surface Recombination Velocity (SB):	100 cm/s

Heavy Doping Effects

Auger Recombination:	considered
Band-gap Narrowing:	Slotboom and De Graaff model is used

Performance Evaluation Results

Open Circuit Voltage (V_{oc})	=	696 mV
Short Circuit Current Density (J_{sc})	=	36.71 mA/cm^2
Fill Factor (FF)	=	0.845
Efficiency (η)	=	21.59%

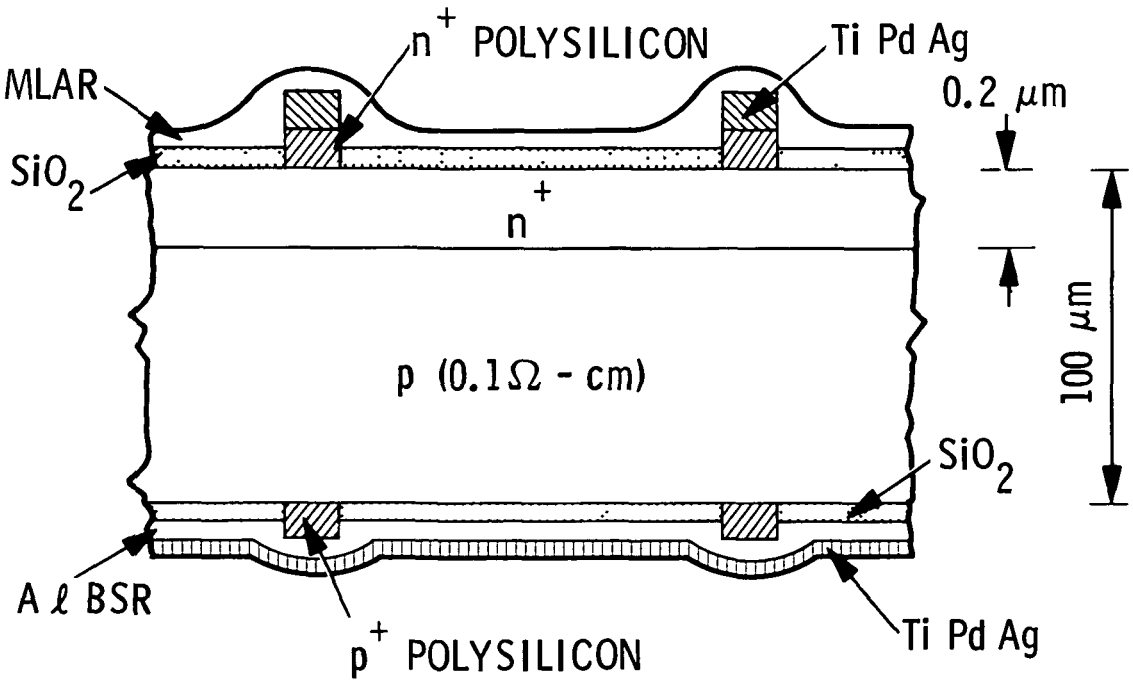

Figure 1. Schematic Cross-Section of a Passivated Thin Silicon Solar Cell Design

Table 2. Effect of Minority-Carrier Lifetime (τ), on Silicon Solar Cell Performance*

τ	V_{oc} (mV)	J_{sc} (mA/cm^2)	FF	Efficiency (%)
1 s	1146	40.59	0.821	38.20
100 ms	1026	40.59	0.818	34.09
10 ms	911	40.59	0.844	31.23
1 ms	831	40.56	0.861	29.02
250 s	793	40.47	0.858	27.55
20 s	730	39.25	0.850	24.33

*NOTE: The following conditions are assumed.
SF = SB = 0 cm/s, Shadowing = 0%.
Auger Recombination and Band-gap Narrowing - not considered.
Geometrical Parameters and Illumination - same as the base case (Table 1).

reduction of τ from 1 ms to 20 μs has caused the efficiency to drop from 29.02% to 24.33%. τ values of the order of 20 μs are experimentally achieved (Reference 1) and higher values of the order of 250 μs may be required for high efficiency cells. Impact of practical barriers is therefore analyzed for the two τ values of interest (τ = 250 μs and τ = 20 μs). Effect of Auger recombination is considered next.

B. AUGER RECOMBINATION

The ideal case described earlier is modified by considering band-to-band Auger recombination in addition to the SRH recombination. All the other parameters are assumed to be the same as for the ideal case. τ for Auger recombination (τ_A) depends quadratically on the doping concentration and is computed by using the empirical relationship of Dziewior and Schmid (Reference 18). Values of τ for SRH recombination (τ_{SRH}) considered are 250 μs and 20 μs. Effective τ (τ_{EFF}) is computed by using the following formula.

$$\frac{1}{\tau_{EFF}} = \frac{1}{\tau_{SRH}} + \frac{1}{\tau_A} \qquad (4)$$

One can see that τ_{EFF} is less than both τ_{SRH} and τ_A and is influenced more by lower of the two values. The solar cell performance results, showing the impact of Auger recombination for the two values of τ_{SRH}, are presented

in Table 3. The Auger effect has reduced the efficiency from 27.55% to 25.18% caused by the drop in V_{oc} from 794 mV to 743 mV. There is no significant difference in J_{sc} or FF for the two cases. This suggests that from Equation 1, the τ_{EFF} for case B is less than 250 μs (influenced by τ_A). Similarly, cases C and D reveal that the effect of Auger recombination, when τ_{SRH} is 20 μs, is marginal; indicating that τ_{EFF} in case D is controlled by τ_{SRH}. It is observed from the results of Table 3 that the amount of impact of Auger recombination is dependent on the relative values of τ_A and τ_{SRH}. As τ_{EFF} is controlled by the lower of the two values, Auger recombination has marginal effect if τ_{SRH} is much less than τ_A. On the other hand if τ_A is less than τ_{SRH}, no matter how large the value of τ_{SRH} is, Auger recombination would have a dominating impact on τ_{EFF} and, hence, cell performance. Effect of band-gap narrowing is considered next.

C. BAND-GAP NARROWING (BGN)

Nonuniform band structure due to heavy doping is considered by Slotboom and De Graaff band-gap narrowing model (Reference 14). It may be noted that the data for p-type silicon is also used for n-type silicon. The cell performance results of considering only BGN (without considering Auger recombination) for the τ_{SRH} values of 250 μs and 20 μs are shown in Table 4. One can observe from Table 4 that impact of BGN is to reduce V_{oc}. For the cases B and D of Table 4 reduction of V_{oc} is about 30 mV, causing the corresponding reduction in efficiency.

Table 5 represents both the individual and combined effects of considering both Auger recombination and band-gap narrowing for τ_{SRH} of 250 μs and 20 μs (discussed in Tables 3 and 4). When both these effects are considered simultaneously (cases D and H), the net effects on V_{oc} and efficiency are obtained by addition of their individual effects on these parameters.

Table 3. Effect of Auger Recombination on Silicon Solar Cell Performance*

Case	SRH	Auger Recombination	V_{oc} (mV)	J_{sc} (mA/cm^2)	FF	Efficiency (%)
A	250 μs	OFF	793.4	40.5	0.858	27.55
B	250 μs	ON	743.0	39.8	0.852	25.18
C	20 μs	OFF	729.9	39.3	0.850	24.33
D	20 μs	ON	720.7	38.7	0.848	23.67

*NOTE: The following conditions are assumed.
SF = SB = 0 cm/s, Shadowing = 0%.
Band-gap Narrowing - not considered.
Geometrical Parameters and Illumination - same as base case (Table 1).

Table 4. Effect of Band-gap Narrowing (BGN) on Silicon Solar Cell Performance*

Case	τ_{SRH}	BGN	V_{oc} (mV)	J_{sc} (mA/cm^2)	FF	Efficiency (%)
A	250 μs	OFF	793.4	40.5	0.858	27.55
B	250 μs	ON	763.0	40.5	0.854	26.37
C	20 μs	OFF	729.9	39.3	0.850	24.33
D	20 μs	ON	699.4	39.3	0.845	23.18

*NOTE: The following conditions are assumed.
SF = SB = 0 cm/s, Shadowing = 0%.
Geometrical Parameters and Illumination - same as base case (Table 1).
Auger Recombination - not considered.

Table 5. Effect of Auger Recombination and Band Gap Narrowing (BGN) on Silicon Solar Cell Performance*

Case	τ_{SRH}	Auger	BGN	V_{oc} (mV)	J_{sc} (mA/cm^2)	FF	Efficiency (%)
A	250 μs	OFF	OFF	793.4	40.5	0.858	27.55
B	250 μs	ON	OFF	743.0	39.8	0.852	25.18
C	250 μs	OFF	ON	763.0	40.5	0.854	26.37
D	250 μs	ON	ON	712.5	39.8	0.848	24.01
E	20 μs	OFF	OFF	729.9	39.3	0.850	24.33
F	20 μs	ON	OFF	720.7	38.7	0.848	23.67
G	20 μs	OFF	ON	699.4	39.3	0.845	23.18
H	20 μs	ON	ON	690.2	38.7	0.848	22.54

*NOTE: The following conditions are assumed.
SF = SB = 0 cm/s, Shadowing = 0%.
Geometrical Properties and Illumination - same as base case (Table 1).

As noticed earlier J_{sc} is affected only by Auger recombination and not by BGN. Effect of surface recombination velocities, with SF and SB having values greater than zero, is considered next.

D. SURFACE RECOMBINATION VELOCITIES (SF, SB)

In this study, both the front and back surfaces are considered to be passivated and both SF and SB are assumed to have the same effective values. For both of them, specific values of 0, 100 and 1000 cm/s are considered. For the two values of τ_{SRH} (250 μs and 20 μs), the cell performance results by varying SF and SB from 0 cm/s to 1000 cm/s, are presented in Table 6. It is observed from the results of Table 6 that there is more than 2 percentage point improvement in efficiency by reducing SF and SB from 1000 cm/s to 100 cm/s (cases B and C) for τ_{SRH} of 250 μs. Correspondingly, there is more than 1.5 percentage point improvement for τ_{SRH} of 20 μs (cases E and F). This shows that passivating both the surfaces is of great importance in achieving higher cell efficiencies. Impact of SF and SB becomes more critical when the τ_{EFF} is very large. It is also observed that reduction of surface recombination losses has an impact on improving both V_{oc} and J_{sc} and, hence, efficiency.

In the above cases, the shadowing effect due to metallization and reflection loss from the front surface are not taken into account. Impact of these parameters is considered next.

Table 6. Effect of Surface Recombination Velocities (SF and SB) *on Silicon Solar Cell Performance**

Case	τ_{SRH}	SF (cm/s)	SB (cm/s)	V_{oc} (mV)	J_{sc} (mA/cm^2)	FF	Efficiency (%)
A	250 μs	0	0	712.5	39.8	0.848	24.01
B	250 μs	100	100	698.0	39.5	0.845	23.28
C	250 μs	1000	1000	660.0	38.1	0.839	21.08
D	20 μs	0	0	690.2	38.7	0.843	22.54
E	20 μs	100	100	683.6	38.5	0.842	22.18
F	20 μs	1000	1000	656.6	37.5	0.838	20.62

*NOTE: The following conditions are assumed.
Shadowing = 0%.
Geometrical Parameters and Illumination - same as base case (Table 1).
Auger Recombination - considered.
Band-gap Narrowing - considered.

E. SHADOWING

In this one dimensional analysis, both shadowing loss due to metallization and optical reflection loss from the front surface are combined together. The metal grid shadowing reduces the surface area. Both these losses together are estimated to be around 7%. By optimal design of contact and use of antireflection coating, this loss may be reduced to about 4%. The effect of shadowing has the direct impact of reducing I_{sc} by the same proportion. V_{oc} is reduced marginally. Reduction in efficiency due to shadowing is therefore proportional to the shadowing factor. In this study three values of shadowing, namely 0, 4 and 7%, are considered. For each case, with a fixed τ_{SRH} value of 250 μs and SF = SB of 0, 100 and 1000 cm/s are considered. The whole set is repeated for τ_{SRH} value of 20 μs. Solar cell performance results for these cases are presented in Table 7 and 8 for τ_{SRH} of 250 μs and 20 μs, respectively. It is observed from Table 7 that, efficiency of 24% corresponding to SF = SB = 0 cm/s, shadow = 0% is reduced to 19.54% corresponding to SF = SB = 1000 cm/s and shadow = 7%, for τ_{SRH} of 250 μs. It is observed that it is essential for SF and SB to have values around 100 cm/s and τ_{SRH} to be around 250 μs for achieving cell efficiency around 22%.

F. BACK SURFACE FIELD (BSF)

In our study with very high τ values and thin cells, the minority carrier diffusion length is greater than the cell thickness. In addition, the substrate is of low resistivity of 0.1 Ω-cm. Under these conditions, the BSF has marginal or no effect on cell performance. This has been verified by numerical analysis.

We have shown in this analysis how the maximum cell efficiency of 30% is reduced to around 19% by considering all the practical barriers. This analysis is performed by using one dimensional numerical analysis technique and using empirical relationships for the constants describing the characteristics of the solar cell. Some of the limitations of the availability of experimental data and the simulation program are discussed in Section IV.

Table 7. Effect of Shadowing (Including Reflection) on Silicon Solar Cell Performance for τ_{SRH} of 250 μs

No.	Case	SF (cm/s)	SB (cm/s)	Shadow (%)	V_{oc} (mV)	J_{sc} (mA/cm^2)	FF	Efficiency (%)
1	A-1	0	0	0	712.5	39.8	0.848	24.01
2	A-2	100	100	0	698.0	39.5	0.845	23.28
3	A-3	1000	1000	0	660.0	38.1	0.839	21.08
4	B-1	0	0	4	711.5	38.2	0.817	23.01
5	B-2	100	100	4	696.9	37.9	0.845	22.31
6	B-3	1000	1000	4	658.9	36.6	0.838	20.20
7	C-1	0	0	7	710.7	37.0	0.847	22.27
8	C-2	100	100	7	696.1	36.7	0.845	21.59
9	C-3	1000	1000	7	658.1	35.4	0.838	19.54

Table 8. Effect of Shadowing (Including Reflection) of Silicon Solar Cell Performance for τ_{SRH} of 20 μs

No.	Case	SF (cm/s)	SB (cm/s)	Shadow (%)	V_{oc} (mV)	J_{sc} (mA/cm^2)	FF	Efficiency (%)
1	A-1	0	0	0	690.2	38.7	0.843	22.54
2	A-2	100	100	0	683.6	38.5	0.842	22.18
3	A-3	1000	1000	0	656.6	37.5	0.838	20.62
4	B-1	0	0	4	689.2	37.2	0.843	21.60
5	B-2	100	100	4	682.5	37.0	0.842	21.25
6	B-3	1000	1000	4	655.4	36.0	0.837	19.76
7	C-1	0	0	7	688.4	36.0	0.843	20.90
8	C-2	100	100	7	681.7	35.8	0.842	20.56
9	C-3	1000	1000	7	654.7	34.9	0.837	19.12

SECTION IV

LIMITATIONS OF THE ANALYSIS

Limitations of the present analysis are discussed under two categories: one concerning the mathematical model used in the present study and the other concerning the lack of experimental data for some of the empirical relationships.

A. SIMULATION PROGRAM

One-dimensional numerical analysis program SCAP1D is used in the present study. Inherently, the cell structure design that can be analyzed should be simple enough so that it can be reduced to a one-dimensional equivalent. Two-dimensional nature of metallization grid design can not be considered without some approximation. Surface recombination velocity, used in the analysis, is assumed to be the effective value representing both that under passivated surface and also that under ohmic contact. Some complicated cell structure designs, such as floating emitter and isolated dot junctions, show promise for achieving high efficiencies. Such designs can not be reduced to their one-dimensional equivalent and, hence, can not be analyzed numerically by any one-dimensional code. Some of the desirable improvements to the program include: inclusion of optical anti-reflection coatings in the code solution, incorporation of texture of the cell, quasi-two-dimensional capability to consider opitimal metallization grid design.

It is also desirable to consider multilevel recombination centers instead of only single level recombination center presently considered. Fermi-Dirac statistics should be incorporated. Carrier-carrier scattering effect on mobility is not considered at present and should be incorporated. Consideration of dislocations and grain boundaries should be included. Hence, it is essential to use a two-dimensional, and in some cases even a three-dimensional, code to analyze complicated solar cell structure designs.

B. LACK OF EXPERIMENTAL DATA

The lack of reliable and accurate experimental data, for the empirical relationships used in the numerical analysis, is a basic problem in accurate evaluation of a given design. Some of the areas of concern are briefly described below.

The empirical formula of Caughey and Thomas for doping dependent mobility is valid for only majority carriers. Because of the scarcity of such data for minority carriers, the same formula is used in the analysis. Slotboom and De Graaff band-gap narrowing model is based on the measurements on p-type silicon. Also, the same data is used for n-type silicon.

There has been some dispute about the accuracy of the Auger recombination coefficients. Detailed experimental study is necessary to establish correct values.

There is no reliable and accurate established technique for measuring surface recombination velocities. Similarly, a technique to accurately determine τ in thin emitters is not available.

Future research should therefore be directed towards improving the numerical analysis technique by expanding its capability to eliminate some of the limitations mentioned above. In addition to this research, effort should also be directed towards measuring reliable and accurate data for the empirical relationships.

Summary of this study is presented in Section V.

SECTION V

SUMMARY

Silicon p-n junction solar cell performance, under 100 mW/cm^2 illumination of a passivated thin cell design (Figure 1 and Table 1), is evaluated using the one dimensional computer simulation program SCAP1D for a number of cases with varying assumptions. Maximum efficiency is estimated with idealized conditions, ignoring both fundamental and technology limited loss mechanisms. Practical barriers such as Auger recombination, band-gap narrowing, non zero surface recombination velocities and non zero shadowing factor, including reflection from the front surface, are considered in succession and their impact is evaluated and quantified.

Maximum efficiency under idealized assumptions is estimated to be 29% using τ_{EFF} of 1 ms, which is comparable with the previously predicted theoretical limit of 30%. Auger recombination and band-gap narrowing, surface recombination and shadowing losses are all assumed to be zero for this case.

Analysis is then performed introducing loss mechanisms sequentially for two values of τ of interest, namely 250 μs and 20 μs. τ_{SRH} of 20 μs is practically achieved and τ_{SRH} of about 250 μs is required for high efficiency cells. Efficiency of about 27% for the ideal case, with τ_{SRH} of 250 μs is reduced to about 20% when τ_{SRH} is reduced to 20 μs and heavy doping effects are considered with surface recombination velocities (SF = SB) of 1000 cm/s. This effect is graphically represented in Figure 2. Shadowing, including reflection, is considered to be 7%, which has the effect of further reducing the efficiency to about 19%; this is comparable with the experimentally achieved limit that is shown on bar C of Figure 3. Figure 3 shows the impact on cell performance for 4% and 7% of shadowing and for SF and SB of 0, 100 and 1000 cm/s.

Technology improvements, to obtain high lifetime materials, have to be combined with sophisticated cell fabrication procedure to reduce effective surface recombination velocity to 1000 cm/s for up to 20% efficiencies, and the 100 cm/s for obtaining up to 22% efficiencies.

Usefulness of numerical analysis technique, in analyzing cell performance and quantifying the impact of practical barriers on cell efficiency, is established. Limitation of the one-dimensional analysis code to evaluate complicated cell designs and the lack of reliable data and measurement techniques is discussed. Need for directing the research efforts in expanding the numerical analysis capabilities, generating the required data and measurement techniques is emphasized.

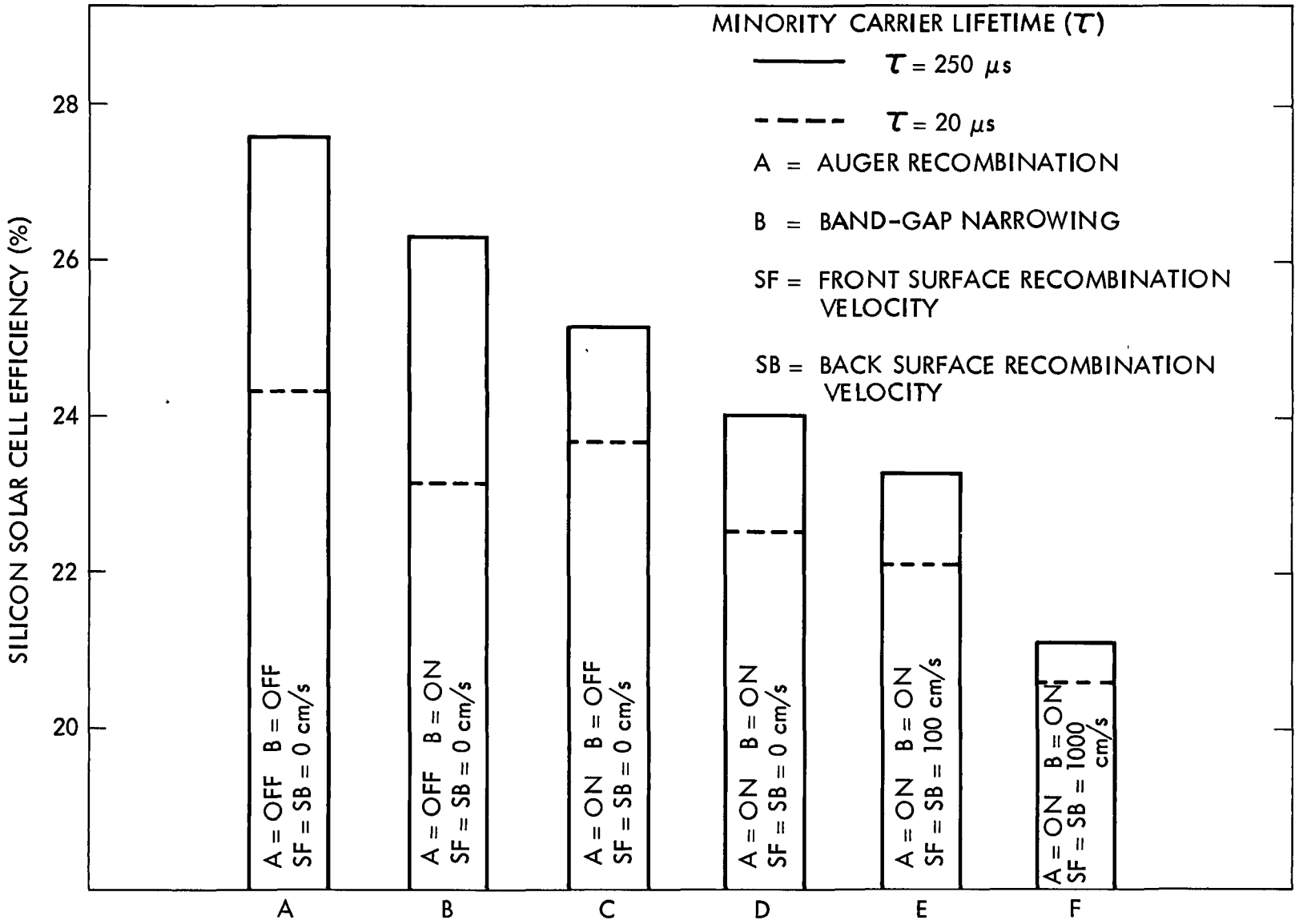

Figure 2. Impact of Practical Barriers on Silicon Solar Cell Performance

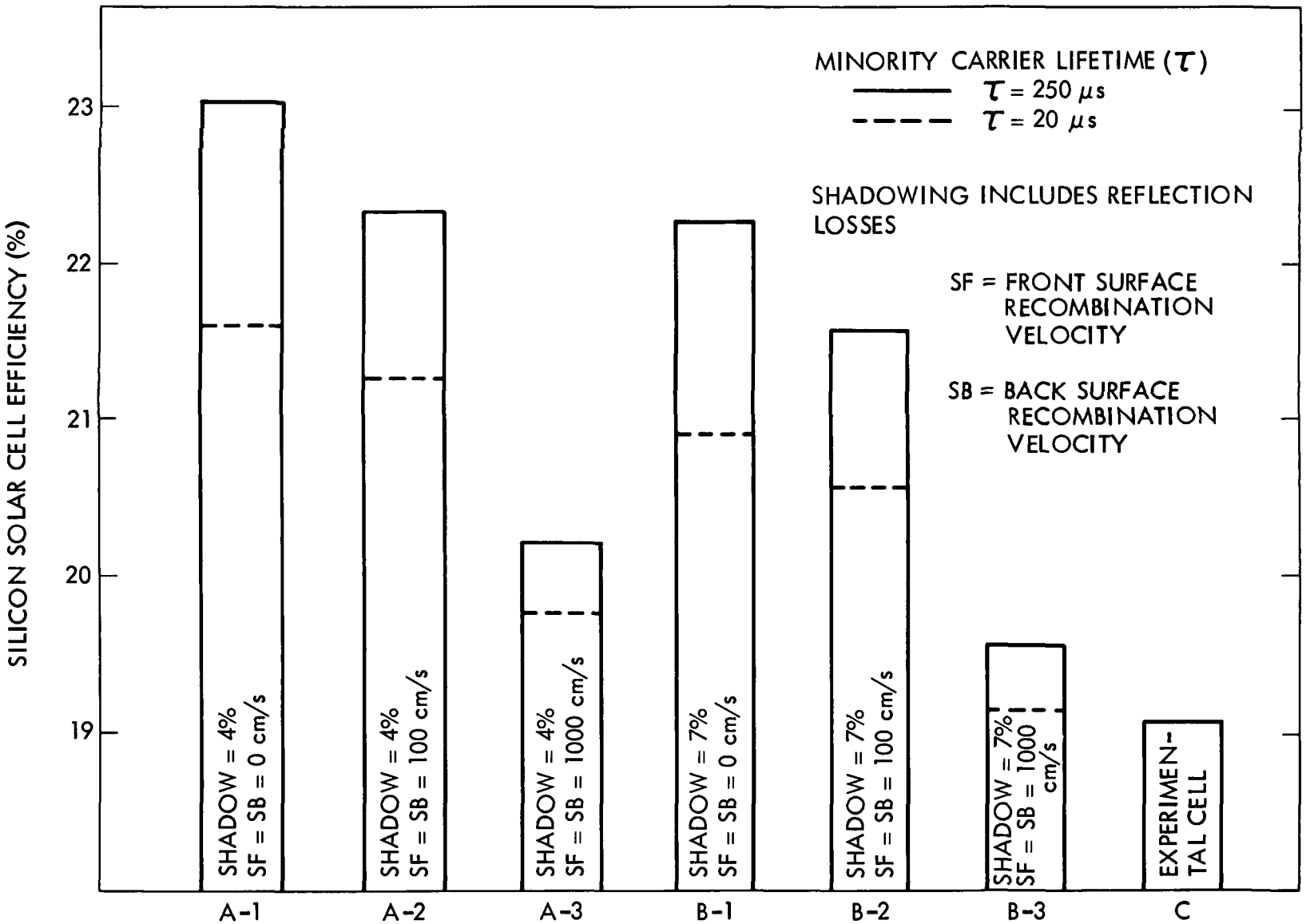

Figure 3. Impact of Shadowing and Surface Recombination Velocities on Silicon Solar Cell Performance

SECTION VI

REFERENCES

1. Green, M.A., Blakers, A.W., Jiqun, S., Keller, E.M., and Wenham, S.R., "High-Efficiency Silicon Solar Cells," IEEE Transactions on Electron Devices, Vol. ED-31, pp. 679-683, May 1984.

2. Green, M.A., Blakers, A.W., Jiqun, S., Keller, E.M., Wenham, S.R., Godfrey, R.B., Szpitalak, T., and Willison, M.R., "Towards a 20% Efficiency Silicon Solar Cell," Seventeenth IEEE Photovoltaic Specialists Conference, pp. 386-389, May 1984.

3. Shockley, W., and Queisser, H.J., "Detailed Balance Limit of Efficiency of p-n Junction Solar Cells," Journal of Applied Physics, Vol. 32, pp. 510-519, March 1961.

4. Rose, A., "Photovoltaic Effect Derived from the Carnot Cycle," Journal of Applied Physics, Vol. 31, pp. 1640-1641, September 1960.

5. Mathers, C.D., "Upper Limit of Efficiency for Photovoltaic Solar Cells," Journal of Applied Physics, Vol. 48, pp. 3181-3182, July 1977.

6. Wolf, M., "How Will We Get To 20% (AM1) Efficient Si Solar Cells?", Sixteenth IEEE Photovoltaic Specialists Conference, pp. 355-360, September 1982.

7. Redfield, D., "Unified Model of Fundamental Limitations on the Performance of Silicon Solar Cells," IEEE Transactions on Electron Devices, Vol. ED-27, pp. 766-771, April 1980.

8. Tiedje, T., Yablonovitch, E., Cody, G.D., and Brooks, B.G., "Limiting Efficiency of Silicon Solar Cells," IEEE Transactions on Electron Devices, Vol. ED-31, pp. 711-716, May 1984.

9. Shockley, W., and Read, W.T., "Statistics of the Recombination of Holes and Electrons," Physical Review, Vol. 87, No. 5, pp. 835-842, 1952.

10. Hall, R.N., "Electron-Hole Recombination in Germanium," Physical Review, Vol. 87, p. 387, 1952.

11. Lundstrom, M.S., "Numerical Analysis of Silicon Solar Cells," School of Electrical Engineering, Purdue University Report TR-EE 80-27, December 1980.

12. Mokashi, A.R., Daud, T., and Kachare, R.H., High Efficiency Silicon Solar Cell Design Evaluation and Sensitivity Analysis, JPL Document 5101-267, JPL Publication 85-46, Jet Propulsion Laboratory, California Institute of Technology, Pasadena, California.

13. Mokashi, A.R., Daud, T., and Kachare, R.H., Sensitivity Analysis of a Passivated Thin Silicon Solar Cell, JPL Document 5101-269, JPL Publication 85-48, Jet Propulsion Laboratory, California Institute of Technology, Pasadena, California.

14. Slotboom, J.W., and De Graaff, H.C., "Measurements of Band Gap Narrowing in Si Bipolar Transistors," Solid State Electronics, Vol. 19, pp. 857-862, 1976.

15. Adler, M.S., "A Method of Achieving and Choosing Variable Density Grids in Finite Difference Formulations and the Importance of Degeneracy and Band-gap Narrowing in Device Modeling," Proceedings of the NASACODE I Conference, Trinity College, Dublin, Ireland, pp. 3-30, 1979.

16. Rajkanan, K., Singh, R., and Shewchun, J., "Absorption Coefficient of Silicon for Solar Cell Calculations," Solid-State Electronics, Vol. 22, pp. 793-795, 1979.

17. Caughey, D.M., and Thomas, R.E., "Carrier Mobilities in Silicon Empirically Related to Doping and Field," Proceedings of the IEEE, Vol. 55, pp. 2192-2193, 1967.

18. Dziewior, J., and Schmid, W., "Auger Coefficients in Highly Doped and Highly Excited Silicon," Applied Physics Letters, Vol. 31, pp. 346-348, 1977.

19. Sah, C.T., "High Efficiency Crystalline Silicon Solar Cells," Second Technical Report, DOE/JPL-956289-84/2, December 1984.